Proceedings of the 25th International Conference on
Port and Ocean Engineering under Arctic Conditions
June 9-13, 2019, Delft, The Netherlands

The effect of floe shape on the interaction of vertical-sided structures with broken ice

Marnix van den Berg[1], Raed Lubbad[1], Sveinung Løset[1]
[1] SAMCoT, Department of Civil and Environmental Engineering,
NTNU, NO-7491 Trondheim

ABSTRACT

In the interaction of broken ice with vertical-sided structures, the ice floe shape can have a significant influence on the ice loads experienced by the structure. The floe shape is especially important in clearance-dominated interaction regimes. This study investigates the effect of floe shape on the clearance-dominated interactions between a vertical-sided circular structure and an unconfined broken ice field. First, the study shows that the floe shape effect exists. Then, the study focusses on the mechanisms responsible for the floe shape effect by comparing aspects of the interaction mechanism between the broken ice field and the structure. The effect of floe shape on the propagation and dissipation of forces in the broken ice field and the effects on the energy dissipation mechanisms are quantified in order to gain more insight in the processes responsible for the floe shape effect. The results show that both the mean value and the standard deviation of ice loads on a vertical-sided structure are higher in a broken ice field with square floe shapes than in a broken ice field with natural floe shapes. The higher mean load appears to be the result of a larger network of force chains in the broken ice around the structure. The force networks seem to have similar properties otherwise.

KEY WORDS Floe shape effect; Energy balance; Broken ice; Force chains

INTRODUCTION

Loads from broken ice can be the design loads for seasonal operations and structures supported by ice management. Broken ice load estimates are often based on the analysis of full-scale data, model-scale experimental data, and/or results from numerical modelling. Parameters that may influence the loads from broken ice on a structure are the ice material properties, the ice areal coverage, the floe size and size distribution, the ice thickness, the floe shape, the ice drift velocity, wind and current conditions, the presence and quantity of ice rubble or brash ice and the confinement conditions. Because of limited available data, the influence of many of the above mentioned parameters is still unclear.

An understanding of the floe shape effect is important in the design of model-scale ice-tank tests and numerical simulations, which are used in the design phase of structures loaded by broken ice. Currently, ice-tank tests with broken ice are often conducted with square or rectangular ice floes (for instance in Haase et al., (2012) and Hoving et al., (2013)). Numerical modelling results indicate that the loads measured in confined broken ice tests with square or rectangular floes may not be representative for the conditions that the test intends to model

(van den Berg et al., 2019). The effect of floe shape in clearance-dominated ice structure interaction has been studied previously by Rheem et al., (1997) and Yamaguchi et al., (1997). However, the model used by Rheem and Yamaguchi is greatly simplified. For example, no floe rotation is taken into account in their model.

A new and extensive study of the effect of floe shape on the ice load experienced by a vertical-sided structure interacting with broken ice is presented in van den Berg et al. (2019). van den Berg et al. (2019) investigates the effect of floe shape in unconfined conditions and in ice-tank tests, where the broken ice field is confined by the tank walls. The primary finding is that the ice floe shape has a large influence on the mean and standard deviation of the ice load in interaction scenarios dominated by ice accumulation and clearance around the structure. The current study presents an extension to the results presented in van den Berg et al. (2019). The differences in ice-structure interaction mechanisms caused by the floe shape effect are studied in more detail by comparing the contributions of different energy dissipation mechanisms and by studying the force propagation and dissipation within the broken ice field.

Interaction between a vertical-sided circular structure and broken ice with an aerial coverage of 70% is modelled with a two-dimensional (2D) Discrete Element Method (DEM). Random broken ice fields are created using 1) floe shapes digitized from a top-view photo of broken sea ice and 2) square floes with the same floe size distribution as the digitized natural floes. The circular structure is propagated for 10 000 m in the randomly created broken ice fields. The ice load on the structure, force propagation and dissipation within the broken ice, and energy dissipation mechanisms are compared for the natural and square broken ice fields, in order to find the causes of the floe shape effect.

SIMULATION METHOD AND SIMULATED CONDITIONS

We study the effect of floe shape using a 2D non-smooth DEM (NDEM) model. The model is an adapted version of the *Simulator for Arctic Marine Structures* (SAMS). SAMS has been used in earlier studies, which are described in Lubbad, et al., (2018a, 2018b); Tsarau et al., (2018); van den Berg, et al., (2018) and van den Berg et al., (2019). The used model is described in detail in van den Berg et al., (2018). Some additional model capabilities related to the treatment of ice-structure contacts are described in van den Berg et al. (2019). In the model, contact forces are calculated implicitly by solving a mixed linear complementarity problem (MLCP) in each time step. The contact geometry and a constant crushing pressure are used to define the force-penetration behaviour at each contact. The force-penetration behaviour is defined based on an assumption of local ice crushing, leading to plastic contact behaviour. The relationship between force and penetration is used in the MLCP to solve the contact forces occurring between interacting bodies. Apart from the contact compliance resulting from this local crushing assumption, all bodies are considered rigid.

The broken ice conditions used in this study are obtained by digitizing a top view photo of a broken sea ice field. Individual floes are detected and digitized using the method described in Zhang & Skjetne, (2015). The digitized broken ice field is visualized in Figure 1. The digitized ice floes have a floe area ranging from 20 m^2 to 4840 m^2. The floe size distribution is shown in Figure 2. Random broken ice fields are created with the same floe size distribution as the digitized broken ice field. One broken ice field is created using the natural floe shapes of the digitized ice floes, and another broken ice field is created in which all floes have a square shape. In both ice fields, floes with the same area are initiated in the same initial positions. After initiation, the overlaps between the floes are resolved before the dynamic simulation is started. This results in similar floe positions for the ice field with natural floe shapes and the ice field with square floe shapes. Apart from the difference in floe shape and the slightly different floe positions, both ice fields are exactly the same.

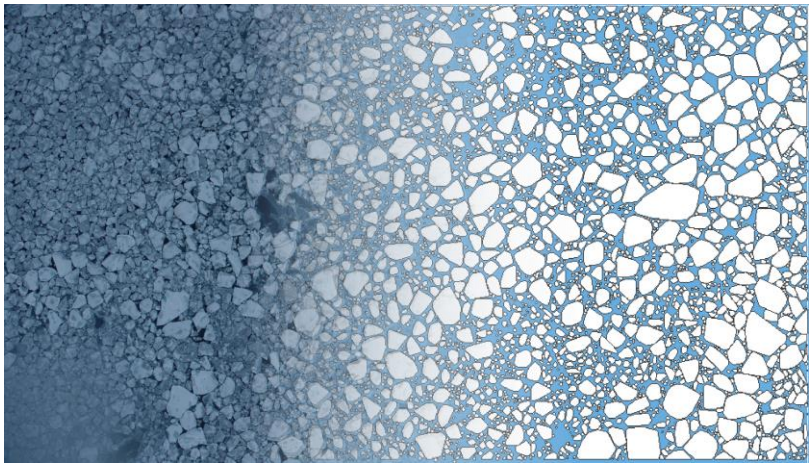

Figure 1. Digitization of a broken ice field from a top view photo. The image merges from photo to digitized ice field from left to right.

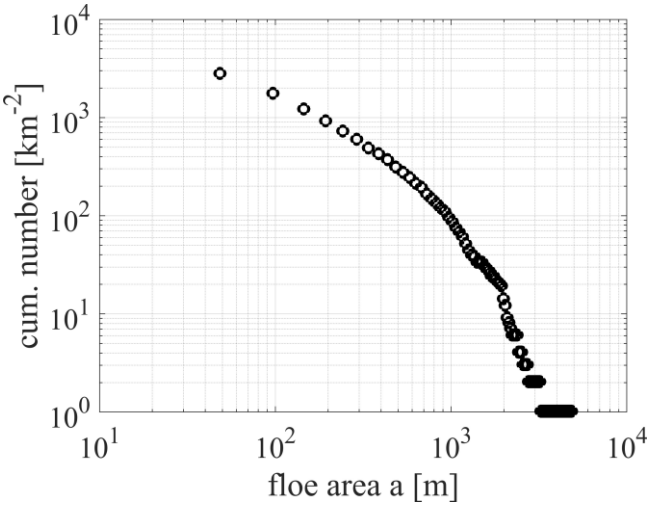

Figure 2. Floe area distribution of the digitized broken ice field.

An interaction length of 10 000 m is simulated for both floe fields. An interaction length of 10 000 m is needed in order to obtain an accurate prediction of the mean load. A domain of 1000 by 900 m around the structure is dynamically simulated. Figure 3 shows the dynamically simulated domain and the structure's position within that domain. The domain size is chosen such that the domain boundaries will not influence the ice load on the structure. The domain is unconfined. Figure 3 also shows the similarity in the floe positions between the broken ice field with natural floe shapes and the broken ice field with square floe shapes. As the structure propagates, floes from the pre-generated floe field that enter the dynamically simulated domain are added. Simultaneously, floes that exit the dynamically simulated domain are removed from the simulation.

Ice splitting failure is implemented following the analytical solutions described by Lu et al., (2015). The contact forces resulting from the DEM simulation are used in each time step to determine if and how an ice floe will split. Because of the 2D nature of the model, ice floe rafting and bending failure is not taken into account. van den Berg et al. (2019) discusses how this simplification may affect the results. Hydrodynamic drag forces resulting from Skin friction and form drag are applied to the ice floes according to their triangulated geometry and the local velocity vector and position of each triangle. The method is described by Tsarau, (2015).

The physical characteristics of the simulated scenarios are given in Table 1. In both scenarios, the structure propagated with a constant velocity in the direction indicated in Figure 3. The structure is fixed in the other degrees of freedom.

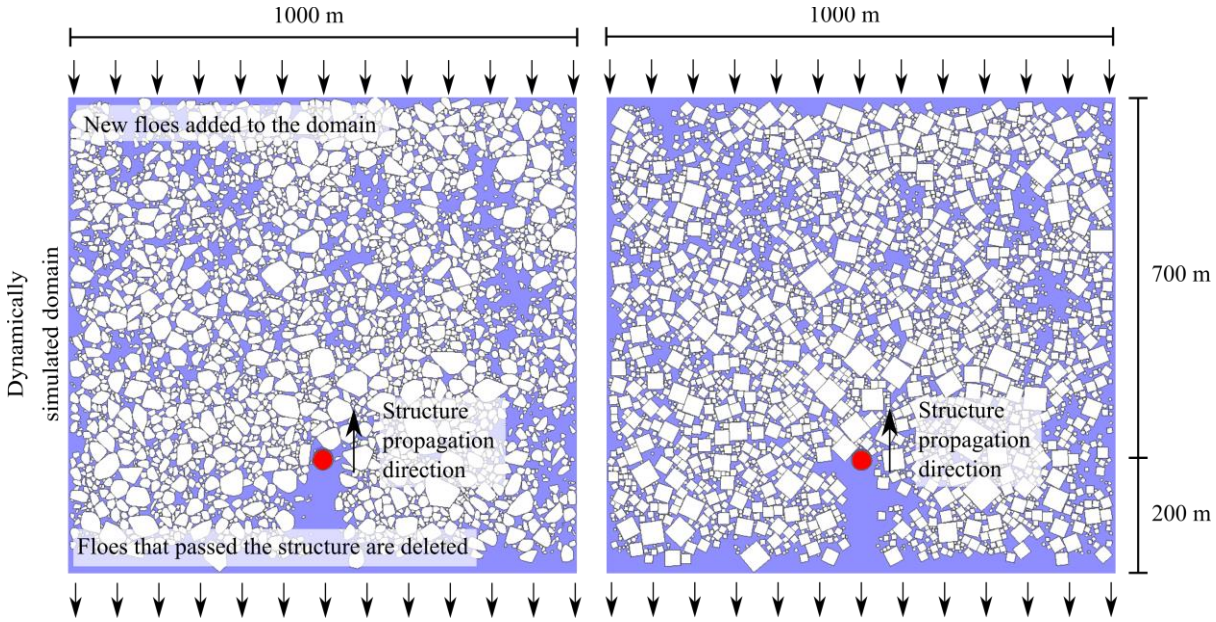

Figure 3. Random broken ice fields created from the digitized broken ice field. Left: natural floe shapes. Right: square floe shapes.

Table 1. Parameters used in the simulations.

Parameter	Value	Parameter	Value
Ice Density	910 kg m^{-3}	Structure diameter	40 m
Ice-ice friction coefficient	0.15	Structure velocity	1.0 m/s
Ice-structure friction coefficient	0.15	Water density	1025 kg m^{-3}
Fracture toughness	150 Pa √m	ice skin friction coefficient	0.005
Crushing pressure	2 MPa	ice form drag coefficient	0.5
Ice thickness	1.0 m	Ice aerial coverage	70 %

RESULTS

We compare the mean value of the ice load, the standard deviation of the ice load, the energy dissipation mechanisms and the size and shape of the force networks within the broken ice in order to identify differences in interaction as a result of the different floe shapes.

Figure 4 shows the mean and the standard deviation of the ice load on the structure (in the direction that is opposite to the structure propagation direction) resulting from the simulations with natural and square floe shapes, respectively. The simulation with natural floe shapes results in a mean ice load of 106 kN and a load standard deviation of 235 kN, while the simulation with square floe shapes results in a mean ice load of 198 kN and a load standard deviation of 398 kN.

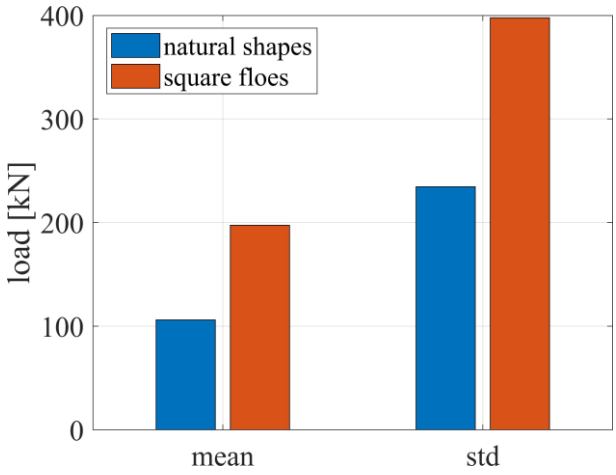

Figure 4. Mean and standard deviation of the ice load on the structure opposite to the structure propagation direction, in the simulation with natural floe shapes and in the simulation with square floe shapes.

We consider the energy balance of the interaction process by comparing the energy input from the structure (ΔE_{str}) and the energy dissipation in the ice field. The latter consists of dissipation in contact normal forces (as a result of local crushing, $\Delta E_{\text{c;n}}$), contact frictional forces ($\Delta E_{\text{c;fr}}$) and hydrodynamic drag (ΔE_{drag}). In addition, there is a small residual energy component resulting from the residual velocity of the ice bodies that are removed from the dynamically simulated domain (E_{res}). In the current implementation of the numerical model, no energy is dissipated in the splitting failure of ice floes. Since the structure is propagated with a constant velocity in both simulations, the energy input from structure propagation is proportional to the mean load from the structure on the ice in the structure propagation direction. Figure 5 shows the energy input and dissipation contributions.

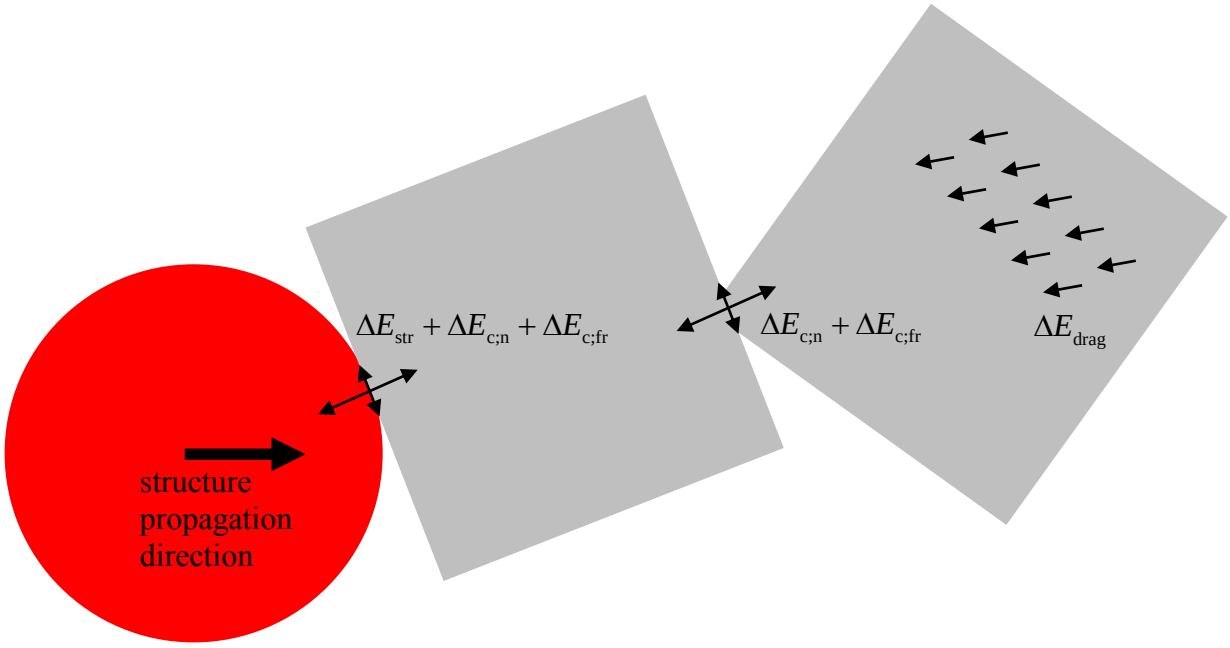

Figure 5. Energy input and dissipation during ice-structure interaction. Energy is introduced in the system by the load component of the ice-structure interaction load in the structure propagation direction. Energy is dissipated in the ice-structure contacts and in ice-ice contacts by contact crushing and friction, and by hydrodynamic drag.

Figure 6 shows the relative contributions of the different energy dissipation mechanisms in the simulation with natural floes and square floes, respectively.

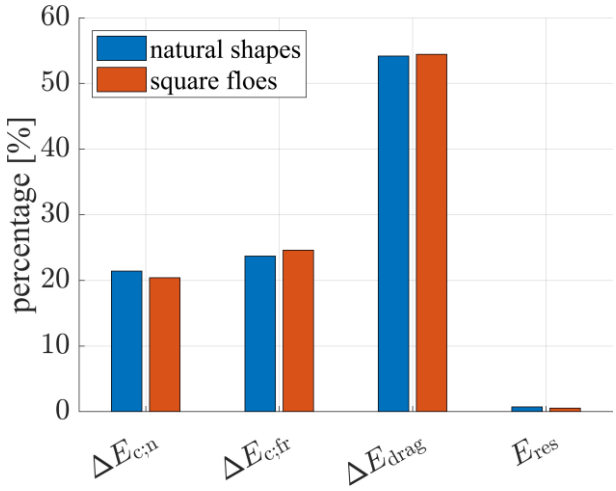

Figure 6. Relative energy dissipation by collisions and drag, natural floe shapes and square floe shapes.

The contributions of the different energy dissipation mechanisms are similar in the natural floe shape simulations and in the square floe shape simulations. In both simulations, 54% of the energy introduced by the moving structure is dissipated by the hydrodynamic drag on the ice floes. The remaining energy is dissipated in the plastic collisions between ice floes and between ice floes and the structure. Frictional contact forces account for a slightly higher proportion of energy dissipation than the normal contact forces. A low proportion of 0.74% (natural) and 0.56% (square) of the introduced energy is removed from the simulation in the form of the residual kinetic energy of bodies that are removed from the simulation domain.

The force propagation and dissipation in the broken ice field is studied both visually and quantitatively. Visual comparison of the simulation results shows that force networks within the broken ice are larger and propagate further from the structure in the simulations with square floes. This results in a higher ice floe area that is accelerated and displaced by the moving structure, leading to a higher ice resistance.

We assign a scalar loading value to each ice floe in order to study the difference in force propagation and dissipation in the broken ice field. The loading value is defined similar to the value used to visualize force chains in Paavilainen & Tuhkuri, (2013), as the maximum eigenvalue of the load tensor $\hat{\alpha}_{ij}$:

$$\hat{\alpha}_{ij} = \sum_{c=1}^{Nc} f_i^c r_j^c \tag{1}$$

in which Nc is the number of contacts of each floe, f_i^c are the contact force vectors, and r_j^c are normalized vectors from the body's centre of gravity to the contact point. Differences in force propagation between the floe fields with natural and square floe shapes are quantified by comparing the mean combined floe area of all floes with a loading value above a range of threshold load values:

$$\overline{A}(F_{thr}) = \frac{\sum_{t=1}^{N_t} A_{\lambda_{max} > F_{thr}}(t)}{N_t} \tag{2}$$

in which $\overline{A}$ is the mean broken ice area with a loading value above threshold load value F_{thr}, N_t is the number of time steps and $A_{\lambda_{\max}>F_{\text{thr}}}(t)$ is the broken ice area with a loading value above load value F_{thr} in each time step.

Figure 7 shows a visual comparison of the force networks occurring in the square floe simulations and the force networks occurring in the real floe simulations. The area of the floes above a load value at a time instance is the summation of the top areas of all coloured floes. A load value of 5 kN is used in the left figures and a load value of 0.25 MN is used in the right figures.

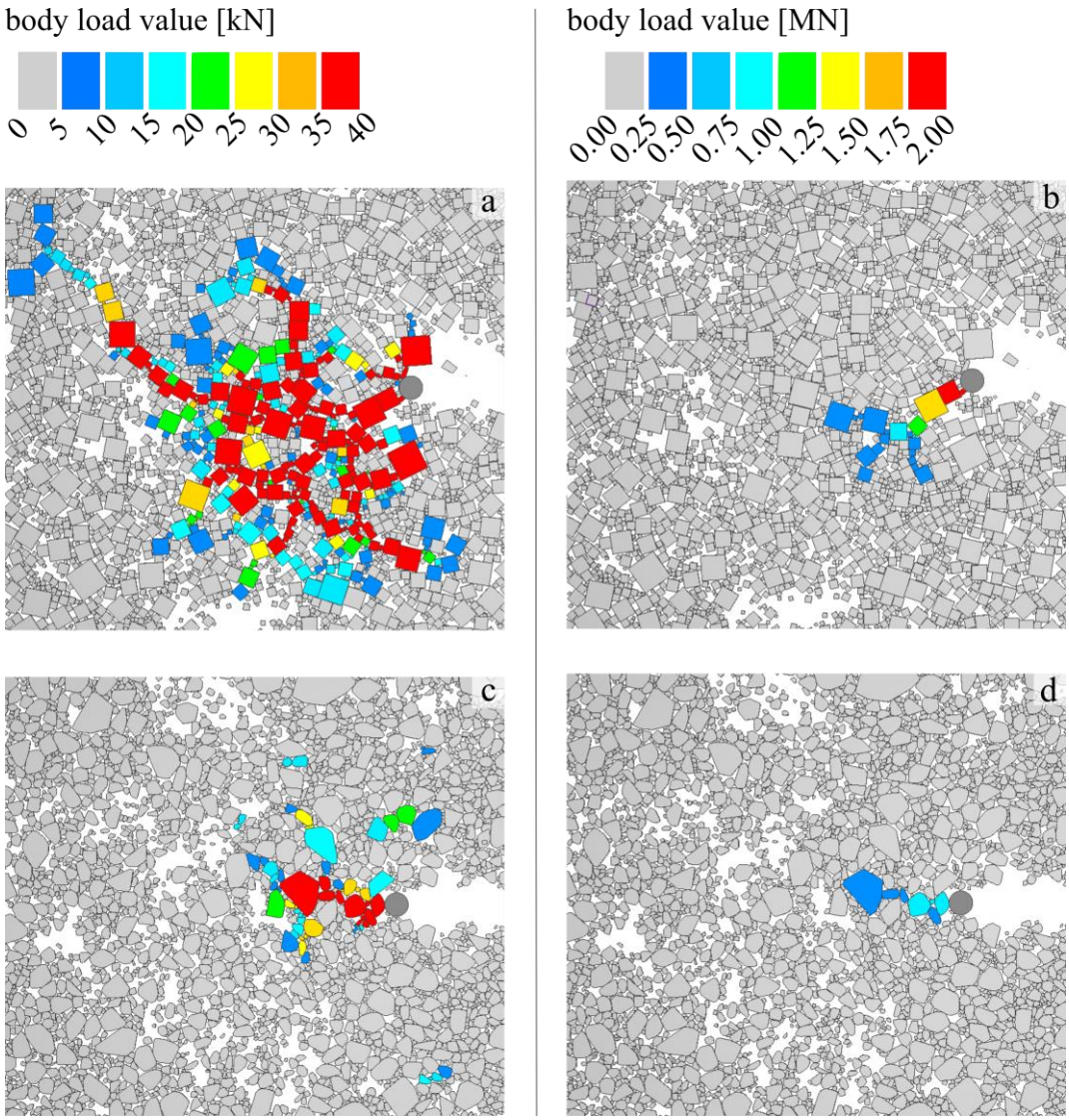

Figure 7. Floes with a load value exceeding a threshold level (coloured floes) for the simulations with square floes (top) and the simulations with natural floe shapes (bottom), and for different threshold levels (left and right).

The resulting load-area curve is shown in Figure 8. Figure 8 shows that the force network is larger in the square floe simulations. Depending on the threshold load level, the mean floe area with a load value higher than the threshold load is 2.15 to 3.13 times higher in the square floe simulations.

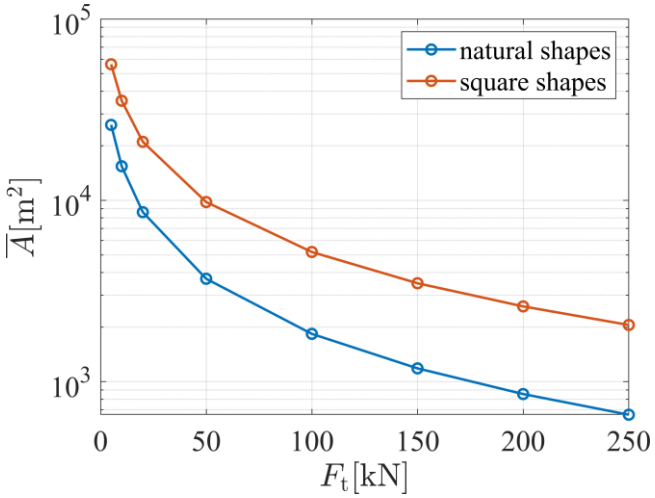

Figure 8. Mean total floe area of the floes exceeding a threshold load level.

DISCUSSION

The mean and standard deviation in the simulation with square floe shapes are almost twice as high as the mean and standard deviation in the simulation with real floe shapes. This difference cannot be explained by comparing the energy dissipation mechanisms. The relative contributions of contact plasticity, friction and drag to the energy dissipation are similar for the simulations with natural and with square floe shapes. Therefore we focus in this section on the force propagation and dissipation behaviour within the broken ice field, in order to clarify the differences between square floe shape and natural floe shape interaction.

In order to gain insight in the differences in force propagation and dissipation, the area-load curved are normalized by scaling the load thresholds with the mean structure load value. The mean area-over-load-threshold as a function of the normalized load thresholds can be described by a power function of the form:

$$\overline{A}(F_{\text{thr}}) = a\left(\frac{F_{\text{thr}}}{\overline{F}_{\text{thr;s}}} + b\right)^{c} + d \tag{3}$$

in which $\overline{F}_{\text{thr;s}}$ is the mean load value of the structure, constants b and c have no units and constants a and d have the unit of m^2. The normalized area-load curves are shown in Figure 9.

The normalized area-load curve of the square floe shape simulation can be scaled to match the area-load curve of the natural floe shape simulation by applying a scaling factor of ~0.7:

$$\overline{A}_{\text{nat}} \approx 0.7\overline{A}_{\text{sq}} \tag{4}$$

The scaled results, as well as a power law fit of the natural and scaled results, are shown in Figure 9. The normalized area-load curve of the natural floe shape simulation and the scaled area-load curve of the square floe simulation can be accurately approximated by the power law function given in Equation (3) with the coefficients $a = 2034$, $b = 0.0127$, $c = -0.891$ and $d = -359.5$. The exact values of coefficient a, b, c and d are not so relevant since they depend on the chosen simulation parameters such as drag and friction coefficients. However, it is an important finding that the normalized area-load curves of both the natural and square floe shape simulations can be approximated with the same power $c = -0.891$. This indicates that the propagation and dissipation processes are similar in the natural and square floe simulations.

The force network in the square floe simulations can be seen as a scaled-up version of the force network in the natural floe simulations.

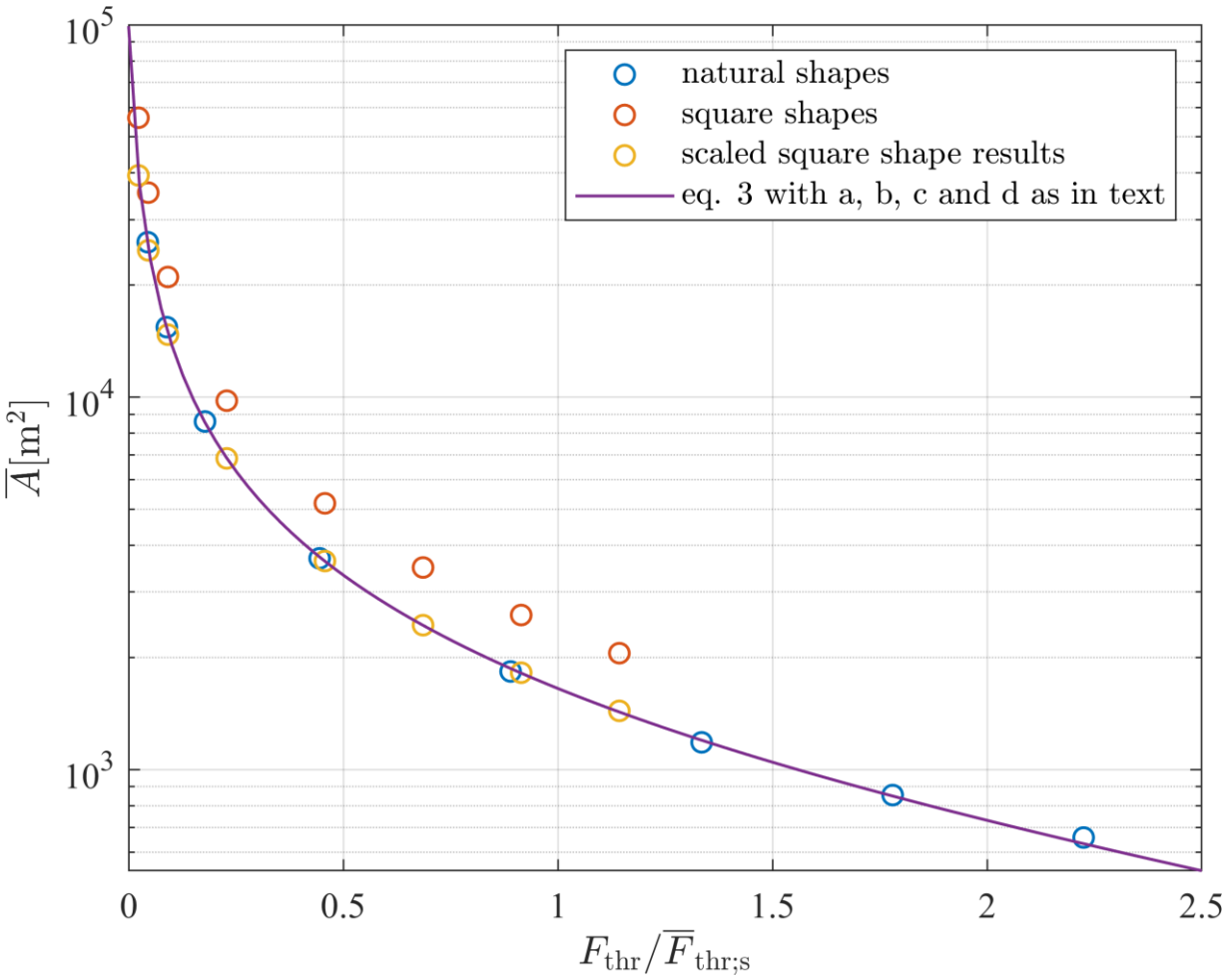

Figure 9. Mean total floe area of the floes exceeding a normalized threshold value, including the scaled square floe results and a power law fit to the natural floe shape and scaled results.

The normalized area-load curve of the natural floe shape simulations can be obtained from the normalized area-load curve of the square floe simulations by applying a scaling factor of ~0.7, while the ratio between the structure load values of the natural and square floe simulations is ~0.51. Based on simple analytical checks considering only hydrodynamic drag forces on the ice floes, we would expect that the normalized area-load curve should scale proportional to the mean structure load values. Clearly, this is not the case.

The reason for the difference between the scaling factor of the area-load curve and the scaling factor of the structure load values is currently unclear. We expect that it is related to the definition of the load value as the maximum eigenvalue of load tensor $\hat{\alpha}_{ij}$. This is supported by the fact that using a different definition of load value leads to a different scaling factor. Using the maximum contact force of each floe in each time step as representative load value leads to a scaling factor of the area-load curve of ~0.8, showing that the scaling factor is dependent on the load value definition. The power c in Equation (3), on the other hand, seems largely independent from the definition of the load value.

Model Limitations

As any numerical model, the model used in this study is a simplification of reality. The simplifications made may influence the modelling results. To investigate the influence of parameter and modelling choices on the simulation results, a sensitivity study was performed by van den Berg et al. (2019). For a further discussion on the influence of modelling and parameter choices on the model results, the reader is referred to this study.

CONCLUSIONS

This study investigates the influence of floe shape on the load experienced by a vertical-sided structure moving through a broken ice field. Numerical simulation results of a simulation with natural ice floe shapes and a simulation with square ice floe shapes are compared. Other than the difference in floe shape, the simulations are identical. The simulation with square floe shapes results in a mean ice load and load standard deviation opposite to the structure propagation direction that is 86% (mean) and 69% (standard deviation) higher than the mean load and standard deviation resulting from the simulation with natural floe shapes.

The energy dissipation mechanisms are similar in the square and natural floe shape simulations. The force networks within the broken ice are larger and propagate further from the structure in the simulations with square floes. This results in a higher ice floe area that is accelerated and displaced by the propagating structure, leading to a higher ice resistance. The force propagation and dissipation behaviour is compared by studying the mean-area-over-load-threshold curves for both simulations. The primary finding is that the normalized area-load curves of the square and natural floe shape simulations can be approximated by a power function with the same power. This indicates that the propagation and dissipation processes are similar in the natural and square floe simulations. The force network in the square floe simulations can be seen as a scaled-up version of the force network in the natural floe simulations.

ACKNOWLEDGEMENTS

The authors would like to acknowledge the support of the SAMCoT CRI through the Research Council of Norway and all of the SAMCoT Partners.

REFERENCES

Haase, A., van der Werff, S., Jochmann, P., 2012. DYPIC - Dynamic Positioning in Ice - First Phase of Model Testing, in: Proceedings of the ASME 2012 31st International Conference on Ocean, Offshore and Arctic Engineering. Rio de Janeiro, pp. 1–8.

Hoving, J.S., Vermeulen, R., Mesu, A.W., Cammaert, G., 2013. Experiment-Based Relations between Level Ice Loads and Managed Ice Loads on an Arctic Jack-Up Structure, in: Proceedings of the 22nd International Conference on Port and Ocean Engineering under Arctic Conditions. Espoo, Finland.

Lu, W., Lubbad, R., Løset, S., 2015. In-plane fracture of an ice floe: A theoretical study on the splitting failure mode. Cold Reg. Sci. Technol. 110, 77–101. doi:http://dx.doi.org/10.1016/j.coldregions.2014.11.007

Lubbad, R., Løset, S., Lu, W., Tsarau, A., van den Berg, M., 2018a. An overview of the Oden Arctic Technology Research Cruise 2015 (OATRC2015) and numerical simulations performed with SAMS driven by data collected during the cruise. Cold Reg. Sci. Technol. 156, 1–22. doi:https://doi.org/10.1016/j.coldregions.2018.04.006

Lubbad, R., Løset, S., Lu, W., Tsarau, A., van den Berg, M., 2018b. Simulator for Arctic Marine Structures (SAMS), in: ASME 2018 37th International Conference on Ocean, Offshore and Arctic Engineering. American Society of Mechanical Engineers, p. V008T07A020-V008T07A020.

Paavilainen, J., Tuhkuri, J., 2013. Pressure distributions and force chains during simulated ice rubbling against sloped structures. Cold Reg. Sci. Technol. 85, 157–174. doi:10.1016/j.coldregions.2012.09.005

Rheem, C.K., Yamaguchi, H., Kato, H., 1997. Distributed mass/discrete floe model for pack ice rheology computation. J. Mar. Sci. Technol. 2, 101–121. doi:10.1007/BF02491524

Tsarau, A., 2015. Numerical Modelling of the Hydrodynamic Effects of Marine Operations in Broken Ice. Norwegian University of Science and Technology.

Tsarau, A., van den Berg, M., Lu, W., Lubbad, R., Løset, S., 2018. Modelling Results With a New Simulator for Arctic Marine Structures-SAMS, in: ASME 2018 37th International Conference on Ocean, Offshore and Arctic Engineering. ASME.

van den Berg, M., Lubbad, R., Løset, S., 2018. An implicit time-stepping scheme and an improved contact model for ice-structure interaction simulations. Cold Reg. Sci. Technol. 155, 193–213. doi:https://doi.org/10.1016/j.coldregions.2018.07.001

van den Berg, M., Lubbad, R., Løset, S., 2019. The effect of ice floe shape on the load experienced by vertical- sided structures interacting with a broken ice field. Mar. Struct. 65, 229–248. doi:10.1016/j.marstruc.2019.01.011

Yamaguchi, H., Rheem, C.K., Toyada, M., Matsuzawa, T., Nakayama, H., Kato, H., Kato, K., Adachi, M., 1997. Influence of Floe Shape on Behaviour of Ice Floes around a Structure, in: OMAE - Volume IV, Arctic/Polar Technology ASME. pp. 461–468.

Zhang, Q., Skjetne, R., 2015. Image processing for identification of sea-ice floes and the floe size distributions. IEEE Trans. Geosci. Remote Sens. 53, 2913–2924. doi:10.1109/TGRS.2014.2366640